ELSEVIER

www.elsevier.nl/locate/ica

Inorganica Chimica Acta 294 (1999) 255–265

Inorganica Chimica Acta

Syntheses and X-ray structures of mixed-metal gold phosphine clusters including an example having a highly asymmetric Re_2Au_2 skeleton

Yoshitaka Katsukawa [a], Satoru Onaka [b,*], Yasuhiro Yamada [b], Masahiro Yamashita [a]

[a] *Division of Informatics for Science, Graduate School of Human Informatics and PRESTO(JST), Nagoya University, Chikusa-ku, Nagoya 464-8601, Japan*

[b] *Department of Environmental Technology, Graduate School of Engineering, Nagoya Institute of Technology, Gokiso-cho, Showaku, Nagoya 466-8555, Japan*

Received 14 January 1999; accepted 2 April 1999

Abstract

This study describes the synthesis and single crystal X-ray characterization of three new heteronuclear gold clusters, i.e. $(OC)_5Re-Re(CO)_4Au_2$dppfe (**1**), $Au_4Co_2(CO)_7(PPh_3)_3$ (**2**), and $[Au-Co(CO)_4]_2$(*cis*-dpen) (**3**). They were synthesized from reaction of $(AuCl)_2$dppfe with $NaRe(CO)_5$ at room temperature, reaction of $(PPh_3)AuCl$ with $NaCo(CO)_4$, and reaction of $(AuCl)_2$-(*cis*-dpen) with $NaCo(CO)_4$, respectively. Compound **1** crystallizes in the monoclinic space group $P2_1/n$ with $a = 15.331(7)$, $b = 23.427(9)$, $c = 13.621(6)$ Å, $\beta = 112.53(3)°$ and $Z = 4$. Compound **2** crystallizes in the triclinic space group $P\bar{1}$ with $a = 12.838(4)$, $b = 22.406(6)$, $c = 11.759(4)$ Å, $\alpha = 103.15(2)$, $\beta = 117.06(2)$, $\gamma = 82.78(2)°$, and $Z = 2$. Compound **3** crystallizes in the triclinic space group $P\bar{1}$ with $a = 10.704(2)$, $b = 17.437(3)$, $c = 10.597(2)$ Å, $\alpha = 96.73(2)$, $\beta = 108.02(2)$, $\gamma = 99.53(2)°$, and $Z = 2$. In **1**, two gold atoms in the Au_2dppfe group are bound to one Re atom in the $Re_2(CO)_9$ group. Thus, the total skeleton is highly asymmetric. The metal skeleton of **2** is composed from a butterfly-like Au_4 backbone with a capping $Co(CO)_3$ group and the terminal $Co(CO)_4$ group coordinated to one Au atom. Two gold atoms come close in **3** to cause intramolecular aurophilic interaction. Terminal $Co(CO)_4$ groups in **2** make an intermolecular pair in a head-to-tail manner in the crystal. © 1999 Elsevier Science S.A. All rights reserved.

Keywords: Gold complexes; Cluster complexes; Phosphine complexes; Crystal structures

1. Introduction

There has been increasing interest in the preparation of mixed-metal clusters that contain gold [1–18], not only because of their potential as bimetallic catalysts [19–21], but also because of their intriguing chemical and physical properties [1,22]. Recently, gold complexes have made another development in the field of supramolecular chemistry where they serve as a building block and/or a linker of component blocks to construct supramolecules [23–29]; in these studies, the role of aurophilic interaction is quite important [30]. We have been interested in the synthesis of nanometer-sized metal clusters by assembling small metal clusters into a suitable spacer and/or a linker [31]; spacer and/or linker molecules employed in these studies were aromatic molecules or phosphine derivatives. In regard to this idea, our attention has recently been directed to the use of gold(I) complexes as a spacer and/or a linker to connect metal clusters in order to construct supramolecules and/or multidimensional arrays of metal clusters in crystals with the aid of aurophilic interaction using the technique of crystal engineering. Indeed we have succeeded to yield a multidimensional array in the single crystal of $(PhS-Au)_2$(μ-*trans*-dpen) (dpen = 1,2-bis(diphenylphosphino)ethylene) by the dual use of Au···Au and π–π interactions [32]. Our next target is to incorporate metal clusters into a Au(I)–

---

* Corresponding author. Tel.: +81-52-735 5160; fax: +81-52-735 5160.

E-mail address: onklustr@ks.kyy.nitech.ac.jp (S. Onaka)

PII: S0020-1693(99)00209-1

phosphine complex to construct a multidimensional array of metal clusters. Therefore, we first have attempted to make a heteronuclear metal–metal bond on a Au(I)–phosphine complex. This paper reports on the syntheses and the crystal structure analyses of three new mixed-metal clusters which contain Au–Re and Au–Co bonds, respectively.

2. Experimental

2.1. General comments

All solvents were purified by standard methods. All reactions were done under argon atmosphere. 1,1′-bis-(diphenylphosphino)ferrocene (dppfe) and *cis*-1,2-bis-(diphenylphosphino)ethylene (*cis*-dpen) were purchased from Strem Chemicals, $Re_2(CO)_{10}$ and $Co_2(CO)_8$ were also purchased from Strem Chemicals. $(AuCl)_2$(μ-dppfe) [33], $(AuCl)_2$(μ-*cis*-dpen) [34], and $(PPh_3)AuCl$ [35] were prepared according to the literature. IR spectra were recorded on a JASCO Valor-III FT-IR spectrometer. Absorption spectra were measured using a JASCO Ubest V-570DS spectrometer. ^{31}P NMR spectra were recorded on a Varian XL-200 spectrometer, the chemical shifts of which were referenced to H_3PO_4.

2.2. Synthesis of complexes

2.2.1. $(OC)_5Re–Re(CO)_4Au_2$dppfe (**1**)

To a THF filtrate (15 ml) of $NaRe(CO)_5$ prepared from 0.10 g (0.14 mmol) of $Re_2(CO)_{10}$ and Na amalgam was added a THF solution (8 ml) of $(AuCl)_2$(μ-dppfe) (100 mg, 0.10 mmol) for 10 min and the mixture was stirred for 28 h at room temperature. The solvent was vacuum-stripped to leave orange–red solid. This solid was washed with a small amount of hexane and the residue was extracted with each 10 ml of benzene five times. The benzene was distilled off from the combined extracts to leave an orange–red solid. This solid was recrystallized from CH_2Cl_2-hexane to give orange crystals. Yield 50 mg (32%). IR (KBr): ν(CO) 2086(w), 2018(m), 1997(s), 1928(s), 1874(s) cm^{-1}. ^{31}P NMR ($CDCl_3$, 298 K): 52.7 (s).

2.2.2. $Au_4Co_2(CO)_7(PPh_3)_3$ (**2**)

A THF solution (40 ml) of $Co_2(CO)_8$ (420 mg, 1.2 mmol) was treated with Na amalgam for 2 h. After the solution was filtered, the THF solution of $NaCo(CO)_4$ was added slowly to an ice-cooled THF solution (80 ml) of $AuCl(PPh_3)$ (888 mg, 1.8 mmol) for 1 h and the mixture was stirred at this temperature for 19 h. The solution changed from yellow to orange–red. The solvent was distilled off at reduced pressure. The residue

Table 1
Crystal data [a]

Compound	$(OC)_5Re–Re(CO)_4Au_2$dppfe (**1**)	$Au_4Co_2(CO)_7(PPh_3)_3$ (**2**)	$[Au–Co(CO)_4]_2$(μ-*cis*-dpen) (**3**)
Formula	$C_{43}H_{28}Au_2FeO_9P_2Re_2$	$C_{61}H_{45}Co_2O_7P_3$	$C_{34}H_{22}Au_2Co_2O_8P_2$
Formula weight	1572.8	1888.6	1132.3
Crystal system	monoclinic	triclinic	triclinic
Space group	$P2_1/n$	$P\bar{1}$	$P\bar{1}$
a (Å)	15.331(7)	12.838(4)	10.704(2)
b (Å)	23.427(9)	22.406(6)	17.437(3)
c (Å)	13.621(6)	11.759(4)	10.597(2)
α (°)	90	103.15(2)	96.73(2)
β (°)	112.53(3)	117.06(2)	108.02(2)
γ (°)	90	82.78(2)	99.53(2)
V (Å^3)	4519(3)	2932(2)	1824.7(6)
Z	4	2	2
$D_{calc.}$ (g cm^{-3})	2.313	2.140	2.062
Crystal dimensions (mm^3)	0.25 × 0.20 × 0.05	0.45 × 0.25 × 0.20	0.45 × 0.40 × 0.20
μ (Mo Kα) (cm^{-1})	55.19	51.34	45.23
Scan type	ω	ω	ω–2θ
Scan range	$1.45 + 0.35 \tan\theta$	$1.50 + 0.35 \tan\theta$	$1.45 + 0.35 \tan\theta$
Scan speed (° min^{-1})	5.0	5.0	5.0
$2\theta_{max}$ (°)	45.0	45.0	55.0
Temperature (K)	298	298	298
Unique reflections	5916	7664	8372
Reflections with $\|F_o\| > 3\sigma(\|F_o\|)$	3430	5871	4820 [b]
Number of parameters refined	538	700	439
R	0.084	0.051	0.121
R_w	0.098	0.039	0.148

[a] Mo Kα radiation ($\lambda = 0.71073$ Å); $R = \Sigma||F_o| - |F_c||/|F_o|$; $R_w = [\Sigma(|F_o| - |F_c|)^2/\Sigma w(F_o)^2]^{1/2}$ where $w = 1/\sigma^2(F)$.

[b] $|F_o| > 6\sigma(|F_o|)$.

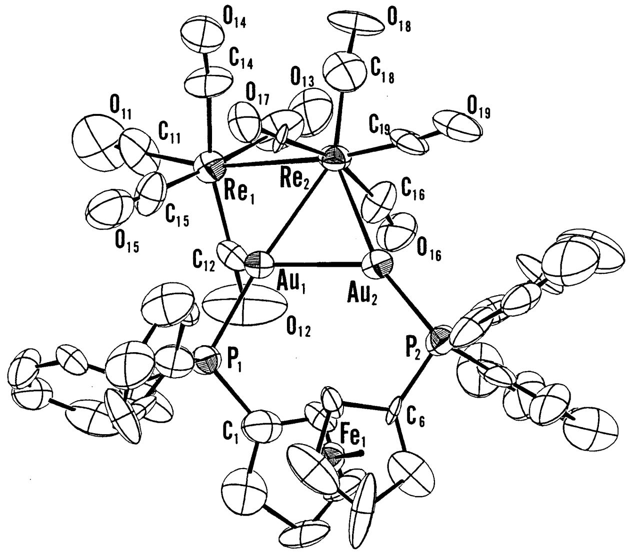

Fig. 1. The ORTEP drawing of $(OC)_5Re-Re(CO)_4Au_2dppfe$ (**1**).

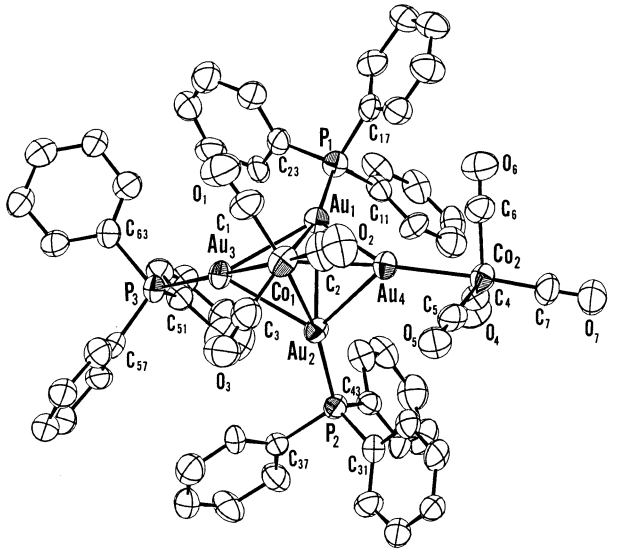

Fig. 2. The ORTEP drawing of $Au_4Co_2(CO)_7(PPh_3)_3$ (**2**).

was dissolved in a minimum amount of benzene and the solution was loaded to a Yamazen medium-pressure liquid chromatograph, YFLC 700 (Waco-gel C-200). The first fraction eluted with benzene was collected. The solvent was vacuum-stripped. The residue was washed with pentane and the dark red residue was extracted with ether. Orange–red crystals were grown from ether to afford 130 mg of **2** (yield, 15%). The main product of this reaction was $Ph_3P-Au-Co(CO)_4$ as was reported by Nyholm and coworkers [36]. IR (Nujol mull): ν(CO) 2054(w), 2042(m), 2033(m,sh), 1984(m), 1960(vs), 1952(vs), 1929(m), 1910(s), 1902(s) cm^{-1}. ^{31}P NMR ($CDCl_3$, 298 K): 39.5(s).

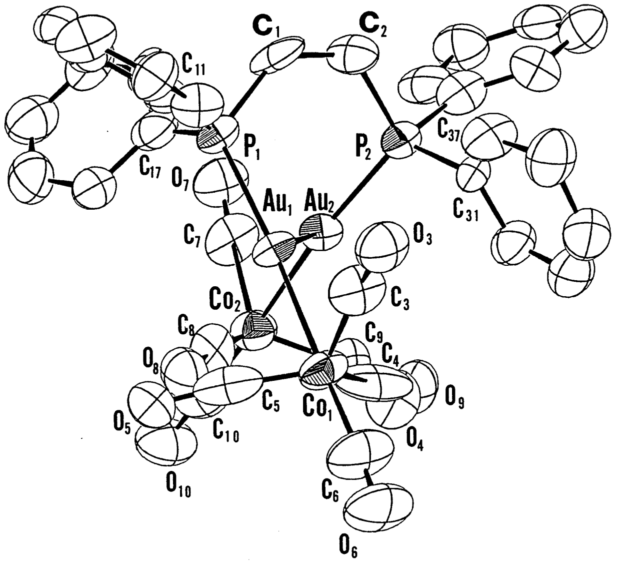

Fig. 3. The ORTEP drawing of $[Au-Co(CO)_4]_2(\mu$-*cis*-dpen) (**3**).

2.2.3. $[Au-Co(CO)_4]_2(\mu$-*cis-dpen) (3)*

A THF solution (25 ml) of $Co_2(CO)_8$ (150 mg, 0.445 mmol) was treated with Na amalgam for 2 h. The THF solution of $NaCo(CO)_4$ thus obtained was transferred to another flask by use of a syringe and to this was added a THF solution (40 ml) of $(AuCl)_2(\mu$-*cis*-dpen) (370 mg, 0.43 mmol). The mixture was stirred at room temperature overnight by covering the reaction vessel with a black cloth. The resulting pale yellow solution was filtered and the solvent was distilled off at reduced pressure. The residue was washed with a small amount of hexane and the brown solid left was recrystallized from hexane–dichloromethane to afford pale yellow single crystals. Yield, 70 mg (14%) in a form of single crystals. IR (Nujol): ν(CO) 2051(s), 1981(s,sh), 1965(vs,sh), and 1945(vs) cm^{-1}. ^{31}P NMR: 17.4.

2.3. *X-ray data collection and crystal structure determination*

All X-ray data were collected by use of a MAC MXC^3 diffractometer equipped with a graphite monochromated Mo Kα radiation ($\lambda = 0.71073$ Å). Crystal data for **1**, **2**, and **3** are collected in Table 1. The structures were solved by direct methods (SIR 92 for **1** and **2** and DIRDIF for **3** in the Crystan-GM program package provided by MAC Science). The structures were refined by a full-matrix least-squares method. All non-hydrogen atoms were refined with anisotropic thermal parameters. The analytical absorption correction was applied at the final stage of refinements [37]. The crystal of **3** showed broad reflections and this property seems responsible for rather high *R* factor. The molecular structures of **1**, **2**, and **3** are shown in Figs. 1–3, respectively. The atomic coordi-

Table 2
The atomic coordinates and isotropic thermal parameters, B_{eq} (Å^2) for **1**

Atom	x	y	z	B_{eq}
Au1	−0.3385(1)	−0.10852(7)	−0.2673(1)	3.77(5)
Au2	−0.2061(1)	−0.12999(7)	−0.3500(1)	4.09(5)
Re1	−0.3459(1)	−0.00309(7)	−0.1385(1)	4.53(5)
Re2	−0.1770(1)	−0.04487(6)	−0.2010(1)	3.45(5)
Fe1	−0.4293(4)	−0.2325(2)	−0.5530(4)	4.0(2)
P1	−0.4613(6)	−0.1751(4)	−0.3329(8)	3.6(3)
P2	−0.2026(7)	−0.1838(4)	−0.4879(8)	3.9(3)
C1	−0.495(2)	−0.182(2)	−0.478(3)	5(1)
C2	−0.463(3)	−0.141(2)	−0.535(4)	6(2)
C3	−0.512(3)	−0.166(3)	−0.646(3)	7(2)
C4	−0.566(4)	−0.223(3)	−0.656(3)	8(2)
C5	−0.560(3)	−0.229(2)	−0.538(4)	7(2)
C6	−0.292(2)	−0.241(2)	−0.524(2)	4(1)
C7	−0.312(3)	−0.271(2)	−0.445(4)	6(1)
C8	−0.386(3)	−0.314(2)	−0.509(6)	8(2)
C9	−0.402(5)	−0.307(2)	−0.617(5)	11(3)
C10	−0.346(3)	−0.262(1)	−0.626(4)	6(2)
C11	−0.426(3)	0.033(2)	−0.079(5)	7(2)
C12	−0.444(3)	−0.006(1)	−0.292(4)	5(1)
C13	−0.298(4)	0.072(2)	−0.181(4)	6(2)
C14	−0.231(3)	−0.002(2)	−0.007(3)	5(1)
C15	−0.372(3)	−0.077(2)	−0.088(3)	5(2)
C16	−0.238(3)	0.002(1)	−0.332(3)	5(1)
C17	−0.149(2)	−0.103(1)	−0.093(3)	4(1)
C18	−0.110(3)	0.023(2)	−0.116(4)	6(2)
C19	−0.070(3)	−0.060(2)	−0.227(3)	4(1)
O11	−0.467(4)	0.053(1)	−0.045(4)	11(2)
O12	−0.500(3)	−0.007(2)	−0.378(4)	11(2)
O13	−0.283(3)	0.114(2)	−0.204(3)	9(2)
O14	−0.170(2)	−0.003(2)	0.072(3)	9(2)
O15	−0.398(3)	−0.115(2)	−0.057(3)	8(1)
O16	−0.283(2)	0.024(1)	−0.406(2)	7(1)
O17	−0.133(2)	−0.133(1)	−0.021(2)	6(1)
O18	−0.065(2)	0.059(1)	−0.071(3)	6(1)
O19	−0.004(2)	−0.067(1)	−0.238(2)	6(1)
C21	−0.575(2)	−0.157(1)	−0.324(3)	3(1)
C22	−0.594(3)	−0.168(2)	−0.229(4)	6(2)
C23	−0.670(2)	−0.149(4)	−0.216(3)	9(2)
C24	−0.729(3)	−0.113(2)	−0.281(4)	6(2)
C25	−0.712(3)	−0.104(2)	−0.377(5)	7(2)
C26	−0.630(2)	−0.116(2)	−0.388(4)	6(2)
C31	−0.430(2)	−0.244(1)	−0.269(3)	4(1)
C32	−0.493(3)	−0.295(3)	−0.287(3)	7(2)
C33	−0.466(3)	−0.343(2)	−0.255(5)	7(2)
C34	−0.379(4)	−0.352(2)	−0.176(4)	6(2)
C35	−0.308(4)	−0.299(2)	−0.144(4)	8(2)
C36	−0.335(2)	−0.258(2)	−0.192(3)	4(1)
C41	−0.234(3)	−0.143(2)	−0.610(3)	5(1)
C42	−0.210(3)	−0.159(2)	−0.690(4)	6(2)
C43	−0.237(4)	−0.125(2)	−0.782(6)	8(2)
C44	−0.282(3)	−0.084(2)	−0.796(4)	7(2)
C45	−0.312(4)	−0.060(3)	−0.714(4)	10(2)
C46	−0.290(4)	−0.092(3)	−0.620(5)	10(3)
C51	−0.085(3)	−0.213(2)	−0.467(3)	5(1)
C52	−0.019(3)	−0.181(2)	−0.467(5)	7(2)
C53	0.075(6)	−0.196(3)	−0.464(8)	11(3)
C54	0.081(4)	−0.238(5)	−0.438(5)	14(4)
C55	0.029(4)	−0.292(3)	−0.426(4)	9(2)
C56	−0.076(3)	−0.271(2)	−0.442(3)	6(2)

Table 3
The atomic coordinates and isotropic thermal parameters, B_{eq} (Å^2) for **2**

Atom	x	y	z	B_{eq}
Au1	0.86988(5)	0.26427(3)	0.92061(6)	4.07(2)
Au2	0.63675(5)	0.23205(3)	0.85559(6)	3.72(2)
Au3	0.68880(6)	0.35730(3)	0.88665(6)	4.04(2)
Au4	0.82977(6)	0.18304(3)	1.04529(6)	4.52(3)
Co1	0.7699(2)	0.30180(9)	1.0770(2)	4.07(8)
Co2	0.8722(2)	0.07210(9)	1.0720(2)	4.65(9)
P1	0.9955(4)	0.2516(2)	0.8252(4)	4.2(2)
P2	0.4803(4)	0.1794(2)	0.6878(4)	3.7(1)
P3	0.6071(4)	0.4187(2)	0.7371(4)	3.9(2)
C1	0.868(2)	0.3606(8)	1.141(2)	5.9(8)
C2	0.824(2)	0.2692(8)	1.216(2)	6.6(8)
C3	0.633(2)	0.3288(8)	1.065(2)	5.3(7)
C4	0.817(1)	0.0640(8)	0.905(2)	5.7(7)
C5	0.774(1)	0.1002(8)	1.140(2)	5.4(7)
C6	1.018(2)	0.0993(8)	1.161(2)	6.0(8)
C7	0.893(2)	−0.0042(8)	1.086(2)	7.5(9)
O1	0.928(1)	0.4034(7)	1.196(1)	9.4(7)
O2	0.854(1)	0.2571(6)	1.317(1)	9.1(6)
O3	0.541(1)	0.3468(6)	1.061(1)	7.2(6)
O4	0.777(1)	0.0554(6)	0.790(1)	7.7(6)
O5	0.711(1)	0.1150(6)	1.189(1)	8.0(6)
O6	1.113(1)	0.1138(7)	1.220(1)	9.3(7)
O7	0.907(1)	−0.0558(6)	1.095(1)	9.8(7)
C11	0.966(1)	0.1870(7)	0.687(1)	4.2(6)
C12	1.003(1)	0.1871(8)	0.590(2)	5.5(7)
C13	0.984(2)	0.1322(9)	0.492(2)	5.7(7)
C14	0.931(2)	0.0825(8)	0.495(2)	6.0(8)
C15	0.897(2)	0.0841(8)	0.591(2)	6.3(8)
C16	0.912(1)	0.1371(8)	0.688(2)	5.8(7)
C17	1.144(1)	0.2344(6)	0.938(1)	4.4(6)
C18	1.238(1)	0.2407(7)	0.913(1)	5.1(7)
C19	1.356(1)	0.2221(8)	0.996(2)	5.4(7)
C20	1.368(1)	0.1951(8)	1.100(2)	6.1(8)
C21	1.275(2)	0.1905(9)	1.121(2)	7.7(9)
C22	1.161(2)	0.2086(8)	1.045(2)	6.0(7)
C23	1.001(1)	0.3176(7)	0.763(2)	4.6(6)
C24	1.084(1)	0.3648(8)	0.851(2)	5.9(7)
C25	1.088(2)	0.4188(8)	0.805(2)	7.6(9)
C26	1.008(2)	0.4235(8)	0.677(2)	6.6(9)
C27	0.926(1)	0.3813(8)	0.596(2)	6.2(8)
C28	0.921(1)	0.3259(7)	0.638(2)	5.2(7)
C31	0.422(1)	0.1285(6)	0.746(1)	4.1(6)
C32	0.504(1)	0.1027(7)	0.852(1)	4.9(6)
C33	0.460(2)	0.0667(7)	0.907(2)	6.3(8)
C34	0.342(2)	0.0541(7)	0.851(2)	5.5(7)
C35	0.262(1)	0.0797(7)	0.743(2)	5.8(7)
C36	0.299(1)	0.1162(7)	0.687(2)	5.4(7)
C37	0.357(1)	0.2310(6)	0.610(1)	3.8(6)
C38	0.343(1)	0.2848(7)	0.691(2)	4.7(6)
C39	0.247(2)	0.3241(8)	0.635(2)	6.8(8)
C40	0.166(2)	0.3101(8)	0.501(2)	6.3(8)
C41	0.183(1)	0.2570(9)	0.425(2)	6.5(8)
C42	0.281(1)	0.2152(8)	0.477(2)	5.5(7)
C43	0.504(1)	0.1336(7)	0.556(1)	3.9(6)
C44	0.595(1)	0.1535(8)	0.536(2)	5.8(7)
C45	0.611(2)	0.1227(9)	0.423(2)	7.2(9)
C46	0.542(2)	0.073(1)	0.341(2)	8(1)
C47	0.459(2)	0.0514(8)	0.365(2)	8(1)
C48	0.439(2)	0.0820(7)	0.473(2)	5.6(7)
C51	0.596(1)	0.3775(7)	0.579(1)	3.8(6)
C52	0.633(1)	0.4024(7)	0.506(1)	4.2(6)

Table 3 (Continued)

Atom	x	y	z	B_{eq}
C53	0.625(1)	0.3648(8)	0.387(2)	5.3(7)
C54	0.577(2)	0.3084(8)	0.339(2)	6.4(8)
C55	0.532(2)	0.2867(8)	0.413(2)	7.9(9)
C56	0.546(2)	0.3188(8)	0.534(2)	6.5(8)
C57	0.460(1)	0.4476(6)	0.708(2)	4.4(6)
C58	0.374(1)	0.4475(7)	0.582(2)	5.0(7)
C59	0.260(2)	0.4757(8)	0.564(2)	7.0(9)
C60	0.239(2)	0.5011(8)	0.670(2)	6.4(8)
C61	0.330(2)	0.4989(8)	0.801(2)	7.1(9)
C62	0.439(2)	0.4706(8)	0.817(2)	6.1(8)
C63	0.691(2)	0.4875(7)	0.776(1)	4.6(6)
C64	0.634(1)	0.5447(7)	0.756(2)	4.9(7)
C65	0.699(2)	0.5947(8)	0.778(2)	5.9(8)
C66	0.818(2)	0.5877(8)	0.820(2)	6.0(8)
C67	0.878(2)	0.5306(8)	0.846(2)	6.7(8)
C68	0.810(2)	0.4809(8)	0.822(2)	5.6(7)

nates are listed in Tables 2–4 and selected bond lengths and angles are tabulated in Tables 5–7.

3. Results and discussion

*3.1. Synthesis and structure of $(OC)_5Re–Re(CO)_4Au_2$-dppfe (**1**)*

The reaction of $(AuCl)_2$(μ-dppfe) with $NaRe(CO)_5$ was first reported by Hor and coworkers several years ago; the product which they isolated from the reaction mixture at −78°C and was characterized by spectroscopic data is $[Au–Re(CO)_5]_2$(μ-dppfe) (**4**) [38]. The product which we obtained in this study from the similar reaction mixture at room temperature exhibits an entirely different IR spectrum in *ν*(CO) region from that of **4**. Therefore, single crystal X-ray analysis has been made; **1** possesses the molecular structure with an unusual asymmetric Re_2Au_2 skeleton as is shown in Fig. 1. One plausible explanation why the product obtained by us is different from that by Hor and coworkers is that **4** produced at low temperature is converted to $(OC)_5Re–Re(CO)_4Au_2$dppfe (**1**) by heat (room temperature). Therefore, we are now planning to synthesize Hor's product at low temperature and to heat the product in solutions.

Table 4
The atomic coordinates and isotropic thermal parameters, B_{eq} (Å^2) for **3**

Atom	x	y	z	B_{eq}
Au1	0.1310(2)	0.2238(1)	0.2300(2)	4.9(1)
Au2	−0.1373(2)	0.2667(1)	0.2805(1)	4.9(1)
Co1	0.2480(6)	0.3207(4)	0.1278(6)	5.0(2)
Co2	−0.3291(6)	0.2579(4)	0.0668(5)	5.2(2)
P1	0.053(1)	0.1212(6)	0.320(1)	3.7(3)
P2	−0.001(1)	0.2907(6)	0.4934(9)	4.4(3)
C1	0.059(5)	0.138(2)	0.486(4)	7(2)
C2	0.058(4)	0.205(3)	0.563(4)	5(1)
C3	0.383(4)	0.309(3)	0.278(5)	6(2)
C4	0.087(5)	0.377(4)	0.149(5)	8(2)
C5	0.210(5)	0.243(4)	0.007(6)	8(2)
C6	0.341(5)	0.390(4)	0.059(5)	8(2)
C7	−0.409(4)	0.198(3)	0.160(5)	5(1)
C8	−0.226(4)	0.226(3)	0.004(4)	5(1)
C9	−0.30(1)	0.359(4)	0.119(6)	13(4)
C10	−0.470(6)	0.246(3)	−0.085(5)	8(2)
C11	0.176(4)	0.051(2)	0.327(3)	4(1)
C12	0.318(5)	0.081(3)	0.358(4)	6(2)
C13	0.393(5)	0.026(3)	0.359(4)	5(2)
C14	0.346(5)	−0.051(3)	0.335(5)	6(2)
C15	0.229(7)	−0.080(3)	0.315(4)	8(2)
C16	0.104(6)	−0.034(3)	0.302(4)	7(2)
C17	−0.085(5)	0.067(2)	0.251(4)	6(2)
C18	−0.192(6)	0.036(2)	0.315(4)	8(2)
C19	−0.310(4)	−0.016(3)	0.258(5)	6(2)
C20	−0.374(5)	−0.039(3)	0.119(5)	7(2)
C21	−0.300(6)	−0.015(3)	0.046(4)	7(2)
C22	−0.146(5)	0.042(3)	0.108(4)	6(2)
C31	0.160(6)	0.367(2)	0.534(4)	6(2)
C32	0.284(5)	0.360(3)	0.608(4)	6(2)
C33	0.415(5)	0.421(3)	0.653(5)	7(2)
C34	0.365(7)	0.491(3)	0.583(5)	8(2)
C35	0.256(6)	0.498(3)	0.509(5)	6(2)
C36	0.136(5)	0.436(3)	0.480(4)	6(2)
C37	−0.047(4)	0.325(3)	0.615(4)	5(1)
C38	−0.013(4)	0.379(3)	0.725(4)	4(1)
C39	−0.052(5)	0.405(3)	0.823(4)	6(2)
C40	−0.214(6)	0.369(3)	0.777(4)	8(2)
C41	−0.301(5)	0.311(3)	0.657(4)	6(2)
C42	−0.211(7)	0.294(3)	0.577(4)	9(2)
O3	0.467(3)	0.309(2)	0.366(3)	7(1)
O4	0.014(3)	0.404(2)	0.142(4)	6(1)
O5	0.134(4)	0.185(2)	−0.102(3)	9(2)
O6	0.395(4)	0.429(2)	0.010(3)	9(1)
O7	−0.447(3)	0.162(2)	0.222(3)	6(1)
O8	−0.132(4)	0.209(2)	−0.046(3)	7(1)
O9	−0.267(4)	0.427(2)	0.159(3)	7(1)
O10	−0.552(3)	0.238(2)	−0.187(3)	7(1)

The molecular structure of **1** is akin to those of $[Au_2Fe_2(CO)_8$(μ-dppm)] (**5**) [39], $[Ru_4H(CO)_{12}B$-{Au_2dppfe}] (**6**) [40], and $[RhRu_3HCp^*(CO)_9B(Au_2$-dppfe)(AuCl)](**7**) [41] but is unusual in that two gold atoms are coordinated to only one Re atom. Two gold atoms make bonds with different Fe atoms and do not bridge two Fe atoms in **5**, two gold atoms are bonded to two different Ru atoms in **6**, and they bridge two Ru atoms in **7**. They all possess intramolecular Au–Au bond(s) and the conformations of Au_2dppfe moieties in **6** and **7** are quite close to that of **1**. The Au1–Au2 distance in **1** is 2.719(2) Å, which is shorter than those in aforementioned **5** (2.915(1) Å), **6** (2.818(2)), **7** (2.850(1) Å), $[Au_4(PPh_3)_4Re(H)_4${P-(p-tol)$_3$}$_2$](BPh_4) (**8**) (2.709–2.829 Å), and $(PhMe_2P)_3$-$ReH_2(AuPPh_3)_3$ (**9**) (2.787(2)–2.812(2) Å). The Re2–Au distances are almost equal (Au1–Re2 = 2.730(2), Au2–Re2 = 2.757(2) Å). These distances are close to those in **8** (2.709–2.741 Å) [2] and slightly longer than those in **9** (2.688(2)–2.730(2) Å) [9]. The distance be-

Table 5
Selected bond lengths (Å) and angles (°) with e.s.d.s in parentheses for **1**

Bond lengths (Å)					
Au1–Re2	2.730(2)	Au2–Re2	2.757(2)	Au1–Au2	2.719(2)
Au1–P1	2.342(9)	Au2–P2	2.28(1)	Re1–Re2	3.175(3)
Re1–C11	1.90(6)	Re1–C12	2.06(4)	Re1–C13	2.07(5)
Re1–C14	1.97(4)	Re1–C15	1.97(4)	Re2–C16	1.99(4)
Re2–C17	1.93(4)	Re2–C18	2.00(5)	Re2–C19	1.85(4)
C11–O11	1.03(9)	C12–O12	1.15(6)	C13–O13	1.10(6)
C14–O14	1.12(5)	C15–O15	1.12(6)	C16–O16	1.11(5)
C17–O17	1.15(5)	C18–O18	1.11(5)	C19–O19	1.22(6)
P1–C1	1.85(4)	P2–C6	1.85(4)		
Bond angles (°)					
Au1–Re2–Re1	61.83(6)	Au2–Re2–Re1	120.14(6)	Au1–Au2–P2	134.5(3)
Au2–Au1–P1	109.7(3)	P1–Au1–Re2	169.8(3)	P2–Au2–Re2	163.4(3)
Au1–Au2–Re2	59.80(6)	Au2–Au1–Re2	60.80(6)	Au1–Re2–Au2	59.40(6)
Au1–P1–C1	109(1)	Au2–P2–C6	112(1)	Au1–Re2–C16	87(1)
Au1–Re2–C17	77(1)	Au1–Re2–C18	145(2)	Au1–Re2–C19	126(1)
Au2–Re2–C16	81(1)	Au2–Re2–C17	89(1)	Au2–Re2–C18	154(2)
Au2–Re2–C19	67(1)	Re1–Re2–C16	85(2)	Re1–Re2–C17	89(1)
Re1–Re2–C18	84(2)	Re1–Re2–C19	172(1)	Re2–Re1–C11	167(1)
Re2–Re1–C12	94(1)	Re2–Re1–C13	77(2)	Re2–Re1–C14	73(2)
Re2–Re1–C15	97(2)				

Table 6
Selected bond lengths (Å) and angles (°) with e.s.d.s in parentheses for **2**

Bond lengths (Å)					
Au1–Au2	2.876(1)	Au1–Au3	2.8672(9)	Au1–Au4	2.805(1)
Au2–Au3	2.870(1)	Au2–Au4	2.7798(8)	Au1–Co1	2.626(3)
Au2–Co1	2.629(2)	Au3–Co1	2.543(2)	Au4–Co1	2.665(2)
Au4–Co2	2.536(2)	Au1–P1	2.306(6)	Au2–P2	2.292(3)
Au3–P3	2.269(4)	Co1–C1	1.73(2)	Co1–C2	1.76(2)
Co1–C3	1.73(2)	Co2–C4	1.73(2)	Co2–C5	1.76(2)
Co2–C6	1.79(2)	Co2–C7	1.73(2)		
Bond angles (°)					
Au1–Au2–Au3	59.86(2)	Au1–Au3–Au2	60.17(2)	Au1–Au2–Au4	59.43(2)
Au1–Au4–Au2	62.00(2)	Au2–Au1–Au3	59.97(2)	Au2–Au1–Au4	58.58(2)
Au3–Au1–Au4	105.83(3)	Au3–Au2–Au4	106.41(2)	Co1–Au1–Au2	56.86(4)
Co1–Au1–Au3	54.93(5)	Co1–Au1–Au4	58.66(5)	Co1–Au2–Au1	56.78(6)
Co1–Au2–Au3	54.86(5)	Co1–Au2–Au4	58.96(4)	Co1–Au3–Au1	57.72(6)
Co1–Au3–Au2	57.73(4)	Co1–Au4–Au1	57.33(6)	Co1–Au4–Au2	57.70(4)
Au1–Co1–Au2	66.36(5)	Au1–Co1–Au3	67.36(7)	Au1–Co1–Au4	64.01(6)
Au2–Co1–Au3	67.40(5)	Au2–Co1–Au4	63.34(4)	Au3–Co1–Au4	120.64(8)
Co2–Au4–Co1	162.72(9)	Co2–Au4–Au1	139.55(8)	Co2–Au4–Au2	128.26(5)
P1–Au1–Au2	138.93(9)	P1–Au1–Au3	124.7(1)	P1–Au1–Au4	128.4(1)
P1–Au1–Co1	163.8(1)	P2–Au2–Au1	140.5(1)	P2–Au2–Au3	126.2(1)
P2–Au2–Au4	126.7(1)	P2–Au2–Co1	162.6(1)	P3–Au3–Au1	130.7(1)
P3–Au3–Au2	127.72(9)	P3–Au3–Co1	170.8(1)		

tween Re1 and Au1 is 3.058(2) Å. This distance is significantly longer than the usual Au–Re bond. In addition, 18-electron rule does not request a covalent bond between Re1 and Au1 atoms. Therefore, we suggest that there is not a strong interaction between Re1 and Au1 atoms. Thus, the Au_2Re skeleton is close to a regular triangle; this is supported from the relevant angles described below. The flexibility of dppfe for coordination to transition metals should make it possible to take such an unusual and crowded structure [42]. The Au–P bond lengths are 2.28(1)–2.342(9) Å. These distances are longer than those of $[Au–Co(CO)_4]_2$(μ-dppfe) (**10**) (2.258(3)–2.262(2) Å) and of $[Au–Mn(CO)_5]_2$(μ-dppfe) (**11**) (2.27(5)–2.28(5) Å) [31e]. The Au1–Re2–Au2 angle and the Au1–Re2–Re1 angle are close to those of the regular triangles of 59.40(6) and 61.83(6)°, respectively. The Re2–Au1–Au2 and Re2–Au2–Au1 angles are 60.80(6) and 59.80(6)°, respectively. The Au2–Re2–Re1 angle is 120.14(6)°. The P1–Au1–Au2 and the P2–Au2–Au1 angles are 109.7(3) and 134.5(3)°, respectively.

Table 7
Selected bond lengths (Å) and angles (°) with e.s.d.s in parentheses for **3**

Bond lengths (Å)					
Au1···Au2	3.265(3)	Au1–Co1	2.482(7)	Au1–P1	2.28(1)
Au2–Co2	2.511(5)	Au2–P2	2.222(9)	C1–C2	1.35(6)
Co1–C3	1.84(4)	Co1–C4	2.17(7)	Co1–C5	1.65(6)
Co1–C6	1.80(6)	Co2–C7	1.80(5)	Co2–C8	1.59(5)
Co2–C9	1.73(6)	Co2–C10	1.80(5)	C3–O3	1.08(5)
C4–O4	0.96(8)	C5–O5	1.38(6)	C6–O6	1.10(8)
C7–O7	1.08(6)	C8–O8	1.33(6)	C9–O9	1.18(7)
C10–O10	1.13(6)	P1–C1	1.73(5)	P2–C2	1.85(5)
Bond angles (°)					
P1–Au1–Co1	169.0(4)	P2–Au2–Co2	164.9(4)	Au1–P1–C1	119(1)
Au2–P2–C2	117(1)	Au1–Co1–C3	76(2)	Au1–Co1–C4	79(2)
Au1–Co1–C5	82(2)	Au1–Co1–C6	177(2)	Au2–Co2–C7	78(1)
Au2–Co2–C8	81(1)	Au2–Co2–C9	84(2)	Au2–Co2–C10	177(1)

*3.2. Synthesis and structure of $Au_4Co_2(CO)_7(PPh_3)_3$ (**2**)*

The reaction of $AuCl(PPh_3)$ with $Co(CO)_4^-$ was first reported by Nyholm and coworkers in 1964 [36]. The product they isolated was the targeted $Ph_3PAu–Co(CO)_4$ (**12**) and the isolation of $Au_4Co_2(CO)_7(PPh_3)_3$ (**2**) was not reported. They produced $Co(CO)_4^-$ anion by reacting $Co_2(CO)_8$ with pyridine in THF and we prepared this anion by reduction of $Co_2(CO)_8$ with Na amalgam. Thus, the cation for Nyholm's synthesis is $[Copy_5]^{2+}$ and the cation in our synthesis is Na^+. This difference in the cation for producing $Co(CO)_4^-$ anion should be responsible for the formation of our cluster.

The molecular structure of **2** is composed of a butterfly-like Au_4 skeleton and triphenyl phosphines and/or a $Co(CO)_4$ group are coordinated to each gold atom as a terminal ligand [8]. The $Co(CO)_3$ group caps the Au_4 skeleton. The skeletal structure looks like a fragment of $Au_6(PPh_3)_4[Co(CO)_4]_2$ (**13**) reported by Velden et al. except the existence of the capping $Co(CO)_3$ group [8] and/or looks like $(dppe)_2Au_3In_3Cl_6(thf)_3$ (**14**) and $[(dppe)_2Au_3In_3Br_7(thf)]^-$ (**15**) reported by Schmidbaur et al. [43]. The Au–Au distances are categorized into two groups, that is, rather long Au–Au distances (2.8672(9)–2.876(1) Å) and short Au–Au distances (2.7798(8)–2.805(1) Å). The latter bonds are concerned with the Au4 atom to which the terminal $Co(CO)_4$ group is bonded. The Au4–Co2 bond (2.536(2) Å) is the shortest among the five Au–Co bonds and the Au3–Co1 bond, which is located at the opposite side to the Au4–Co2 bond, is the next short Au–Co bond (2.543(2) Å). Among four Co1–Au bond lengths, the Co1–Au3 bond length is the shortest (2.543(2) Å) and the Co1–Au4 is the longest (2.665(2) Å). Among five Au–Au bond lengths, those concerned with Au4 atom, that is, Au4–Au1 and Au4–Au2 bond lengths are significantly shorter than those of Au1–Au2, Au1–Au3, and Au2–Au3 bond lengths. The Au4–Co2 bond length is longer than those of **12** (2.50(1) Å) [36], **10** (2.492(1)–2.499(1) Å) [31e], and **13** (2.46(2) Å) [8]. The Au–P bond lengths (2.269(4)–2.306(6) Å) are almost in the same range as those of **13** (2.28(4)–2.37(2) Å) [8]. The Au3–Au1–Au4 angle is 105.83(3)° and the Au3–Au2–Au4 angle is 106.41(2)°. The Au–Au–Co(capping) angles are classified into three groups, that is, the groups around the 59° (Co1–Au1–Au4 and Co1–Au2–Au4), the groups around 55° (Co1–Au1–Au3 and Co1–Au2–Au3), and the groups around 57° (Co1–Au1–Au2, Co1–Au2–Au1, Co1–Au3–Au1, Co1–Au3–Au2, Co1–Au4–Au1, and Co1–Au4–Au2). The fact that the capping $Co(CO)_3$ group is slightly leaned to the Au3 atom is substantiated by comparisons of these bond angles and the Co1–Au bond lengths mentioned above. The $Co(CO)_4$ group has the similar slightly distorted trigonal bipyramidal coordination as those of **10**, **12** and **13**. In order to assimilate these core structural features, two propositions are presented; firstly the 18-electron rule suggests that the $Co(CO)_4$ group is an anion and the capped $Co(CO)_3$ group should be a cation if four Co1–Au bonds are assumed. Thus the cationic charge on Co1 is cancelled by the anionic charge on the terminal $Co(CO)_4$ group to make the cluster neutral. Second proposition is that the capping $Co(CO)_3$ group makes three Au–Co bonds between Co1 and Au1, Au2, and Au3, respectively, but there is no bond between Co1 and Au4. In addition the terminal $Co(CO)_4$ is an anion and Au4 is a cation to make the cluster neutral. The latter interpretation is based on the facts that (1) the Co1–Au4 bond is the longest among the four Co1–Au bonds and the Au4–Au1 and Au4–Au2 bonds are shorter than Au3–Au1 and Au3–Au2 bonds and (2) the ^{197}Au Mössbauer spectrum and a LCGTO-DF method calculation on the Mulliken charge of Au atoms for **14** and **15** which have quite similar core structures to the present cluster have shown that the Au atom in a similar corner position can be assigned oxidation state +1 and other Au atoms are assigned oxidation state 0 [43]. However, the Co1–Au4 bond is not longer enough than Co1–Au1 and Co1–Au2 bond (only 0.04 Å longer) to neglect the bond between Co1 and Au4 atoms. Therefore, this issue must wait for future spectroscopic study such as XPS and/or ^{197}Au Mössbauer measurements.

*3.3. Synthesis and structure of [Au-Co(CO)$_4$]$_2$(μ-cis-dpen) (**3**)*

The title compound was obtained as was aimed by reacting $NaCo(CO)_4$ with $(AuCl)_2$(μ-*cis*-dpen) in THF with 2:1 mole ratio. The maintenance of the *cis*-configuration in **3** is amazing, because $(Au-X)_2$(μ-*cis*-dpen) (X = Cl, Br, I, and *p*-$SC_6H_4CH_3$) is isomerized easily to $(Au-X)_2$(μ-*trans*-dpen) in solutions [45]. Thus, the two Au atoms come close in the molecule (the Au–Au distance is 3.265(3) Å) to suggest an intramolecular aurophilic interaction [32]. The intramolecular Au–Au distance in $(AuCl)_2$(μ-*cis*-dpen) is 3.05(1) Å [44]. Thus, the aurophilic interaction is reduced by replacing the Cl anions with $Co(CO)_4$ groups. The Au–Co bond lengths are 2.482(7) and 2.511(5) Å, which are in the same range of Au–Co bonds in **10** [31e]. The *cis*-dpen group is concluded to afford almost the same electronic effect on the Au–Co bond as that of dppfe. The P–Au–Co bonds are slightly distorted from linearity (169.0(4) and 164.9(4)°). The steric repulsion that resulted from the *cis* configuration may be responsible for the distortion from the linearity. Although two Co atoms are not in the close proximity (the intramolecular Co–Co distance is 5.04(1) Å), some CO groups coordinated to these cobalt atoms come close in the molecule (3.3(1)–3.47(7) Å), but they are not parallel in the molecule.

*3.4. Crystal structures of **1**, **2**, and **3***

As described in the introduction, we are very much interested in the crystal packing of these clusters for possible unveiling of the intermolecular Au–Au interaction. Although drawings of crystal packings for these clusters do not indicate such an aurophilic interaction in the crystals, an interesting intermolecular pair formation in a head-to-tail manner is detected for the terminal $Co(CO)_4$ groups of **2**. Fig. 4 displays the crystal packing of the cluster **2** along the *c* axis and the pair formation is indicated by circles. The nearest contact in this pair is 3.46(3) Å (C6···O7). In the previous paper, we have found that similar pairs are formed in the crystal among the neighboring $Co(CO)_4$ groups in [Au-Co(CO)$_4$]$_2$(μ-dppfe) (**10**) and the peaks observed for solid samples are doubled with expected numbers of peaks ($2A_1 + E$) under a C_{3v} local symmetry for **10** [31e]. We have concluded that the doubling is the result of the splitting of each peak and such a pair formation in a head-to-tail manner is responsible for ν(CO) splitting by intermolecular dipole–dipole interaction in solid states. The IR spectrum of a Nujol mull sample of **2** is shown in Fig. 5a and that of a benzene solution sample is shown in Fig. 5b; the KBr disk sample shows a similar IR spectrum as that of a Nujol mull sample. Apparently the peak at 2032 cm^{-1} for the solution sample splits into two peaks (2042 and 2033 cm^{-1}) for the Nujol mull sample. Similar splitting is observed for the peaks at 1955 cm^{-1} (1960 and 1952 cm^{-1}) and 1916 cm^{-1} (1910 and 1902 cm^{-1}). The peaks observed for the solution sample at 2054 and 1984 cm^{-1} are observed as a single peak at 2054 and 1984 cm^{-1}, respectively for the Nujol mull sample. The weak peak at 1929 cm^{-1} observed for the Nujol mull sample should be hidden behind the shoulder of the main peak at 1955 cm^{-1} for the solution sample. Thus, the ν(CO) peaks are classified into two groups, that is, the group of 2032(w), 1955(vs), and 1916(m) cm^{-1} and the group of 2054(s), 1984(s), and perhaps 1929 cm^{-1} (read from the spectrum of the solid sample). The terminal $Co(CO)_4$ group has a C_{3v} local symmetry and the capping $Co(CO)_3$ group has a C_s local symmetry. Therefore, the $Co(CO)_3$ group is also expected to show three ($2A' + A''$) IR-active vibrations. The assignment that the CO vibrations in the terminal $Co(CO)_4$ group contribute mainly to the former peaks is rationalized if the same reasoning for the splitting is applicable to the IR spectrum of the solid sample of **2**. Under this

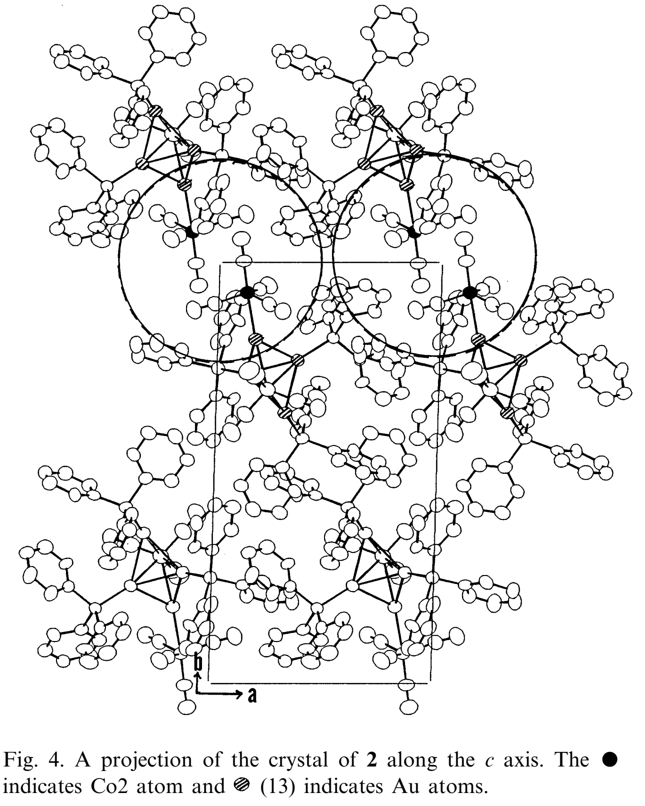

Fig. 4. A projection of the crystal of **2** along the *c* axis. The ● indicates Co2 atom and ◍ (13) indicates Au atoms.

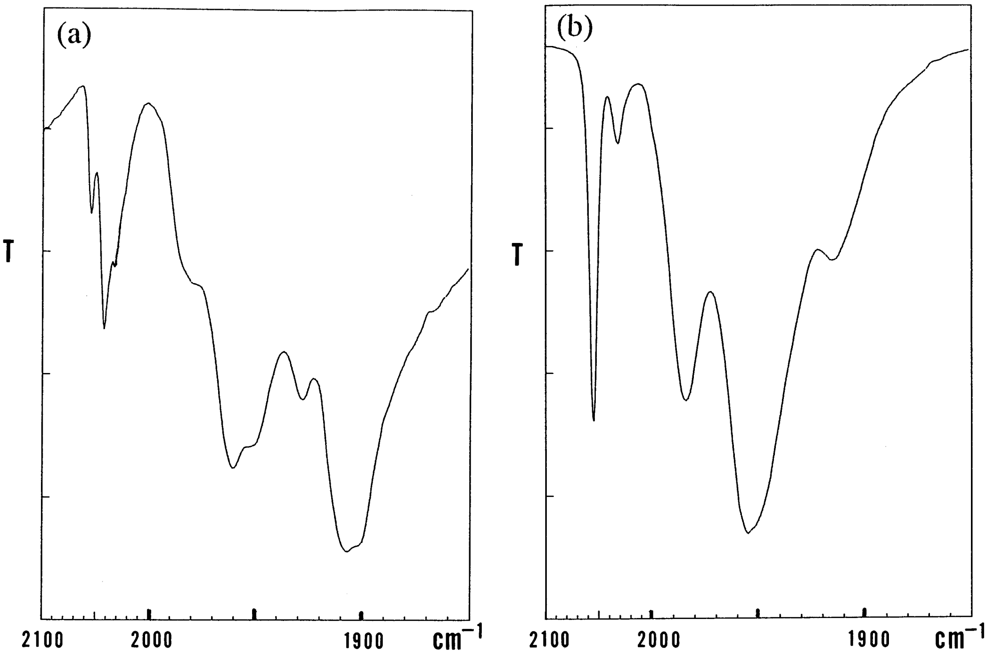

Fig. 5. (a) IR spectrum of **2** in the ν(CO) region for a Nujol mull sample. (b) IR spectrum of **2** in the ν(CO) region for a benzene solution.

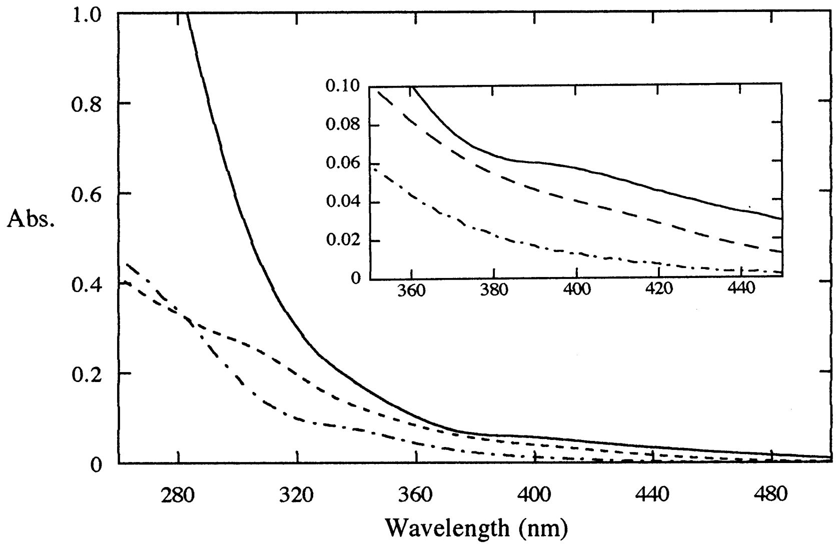

Fig. 6. Absorption spectra of **1** (—), **2** (----), and **3** (--·--·) in a CH_2Cl_2 solution at room temperature. Inserted Figure: absorption spectra for expanded scale of absorbance in the 350–450 nm region.

assignment, these vibrations (2032, 1955, and 1916 cm^{-1}) are just in-between for those of **12** (2045, 1975, and 1945 cm^{-1}) and **13** (2010, 1940, and 1885 cm^{-1}). Thus, the electron density on the metal skeleton of **2** is deduced to be lower than that of **13** and higher than that of **12** [8].

*3.5. Spectroscopic data of **1**, **2**, and **3***

The ^{31}P NMR spectrum shows a single resonance at δ 52.7 for **1** in $CDCl_3$, which suggests that the molecular structure of **1** is maintained in solutions. The ^{31}P-nuclei of **1** resonate in significantly lower field compared with that of **10** (32.36) where Au atoms are bonded to Co atoms [31e], but is close to those of **4** (53.58), **8** (55.3), and **9** (57.3) where Au atoms are bonded to Re atoms. The ^{31}P NMR spectrum of **2** shows a sharp signal at δ 39.5 at room temperature. This is peculiar if the solid-state core structure is maintained in a solution. A rational interpretation is that the Co1–Au4 bond is cleaved in a solution to produce a pseudo C_{3v} symmetry species with the $CoAu_3(PPh_3)_3$ core. The ^{31}P NMR spectrum of **3** shows a peak at δ 17.4, which is significantly shifted to a higher field compared with that of **2** and **10**. Intramolecular Au···Au interaction may be responsible for this high field shift.

All the clusters synthesized in this work are light-yellow to orange–red. The absorption spectra of these new clusters at wavelengths greater than 260 nm are displayed in Fig. 6. The orange–red complex **1** displays a weak absorption at 390 and the orange–red complex **2** shows weak peaks at 300 and 400 nm, while the pale-yellow complex **3** shows a weak absorption at 335 nm. These absorptions are assigned tentatively due to gold(I)–gold(I) interaction(s) based on the recent interpretation for $[Au_3(dppm)_2X_2]X$ complexes by Che and coworkers [46], because all these compounds possess gold(I)–gold(I) interactions.

4. Supplementary material

The $|F_o| - |F_c|$ tables and anisotropic temperature factor tables are available from the author (S.O.).

Acknowledgements

This work was supported by Iketani Science and Technology Foundation and Grant-in Aids for Scientific Research on Priority Areas (No. 10149221 'Metal-assembled Complexes') from Ministry of Education, Science, Sports, and Culture, Japan.

References

[1] K.P. Hall, D.M.P. Mingos, Prog. Inorg. Chem. 32 (1984) 237. C.E. Briant, K.P. Hall, D.M.P. Mingos, J. Chem. Soc., Chem. Comm. (1983) 843. D.M.P. Mingos, R.W.M. Wardle, J. Chem. Soc., Dalton Trans. (1986) 73. C.E. Briant, D.I. Gilmore, D.M.P. Mingos, J. Chem. Soc., Dalton Trans. (1986) 835. S.G. Bott, D.M.P. Mingos, M.J. Watson, J. Chem. Soc., Chem. Comm. (1989) 1192. R.C.B. Copley, D.M.P. Mingos, J. Chem. Soc., Dalton Trans. (1996) 491 and references therein.

[2] B.D. Alexander, B.J. Johnson, S.M. Johnson, A.L. Casalnuvo, L.H. Pignolet, J. Am. Chem. Soc. 108 (1986) 4409. P.D. Boyle B.J. Johnson, A. Buehler, L.H. Pignolet, Inorg. Chem. 25 (1986) 5. P.D. Boyle, B.J. Johnson, B.D. Alexander, J.A. Casalnuvo, P.R. Gannon, S.M. Johnson, E.A. Larka, A.M. Mueting, L.H. Pignolet, Inorg. Chem. 26 (1987) 1346. B.D. Alexander, P.D. Boyle, B.J. Johnson, J.A. Casalnuvo, S.M. Johnson, A.M. Mueting, L.H. Pignolet, Inorg. Chem. 26 (1987) 2547. P.D. Boyle, D.C. Boyd, A.M. Mueting, L.H. Pignolet, Inorg. Chem. 27 (1988) 4424. L.N. Ito, B.J. Johnson, A.M. Mueting, L.H. Pignolet, Inorg. Chem. 28 (1989) 2026. L.N. Ito, A.M.P. Felicissimo, L.H. Pignolet, Inorg. Chem. 30 (1991) 387 and references therein.

[3] P. Braunstein, H. Lehner, D. Matt, A. Tiripicchio, M. Tiripicchio-Camellini, Angew. Chem., Int. Ed. Engl. 23 (1984) 304. P. Braunstein, J. Rosé, A.M. Moanotti-Lanfredi, E. Sappa, J. Chem. Soc., Dalton Trans. (1984) 1843.

[4] C.E. Housecroft, A.L. Rheingold, Organometallics 6 (1987) 1332. J.R. Galsworthy, C.E. Housecroft, A.L. Rheingold, J. Chem. Soc., Dalton Trans. (1995) 2639. J.R. Galsworthy, C.E. Housecroft, A.L. Rheingold, J. Chem. Soc., Dalton Trans. (1996) 2917.

[5] M. Green, K.A. Mead, R.M. Mills, I.D. Salter, F.G.A. Stone, P. Woodward, J. Chem. Soc., Chem. Comm. (1982) 51. L.W. Bateman, M. Green, J.A.K. Howard, K.A. Mead, R.M. Mills, I.D. Salter, F.G.A. Stone, P. Woodward, J. Chem. Soc., Chem. Comm. (1982) 773. L.J. Farrugia, M.J. Freeman, M. Green, A.G. Ortepn, F.G.A. Stone, I.D. Salter, J. Organomet. Chem. 249 (1983) 273. J.E. Goldberg, D.F. Mullica, E.L. Sappenfield, F.G.A. Stone, J. Chem. Soc., Dalton Trans. (1992) 2495.

[6] R.P.F. Kanters, J.J. Bour, P.P.J. Schlebos, J.J. Steggerda, J. Chem. Soc., Chem. Comm. (1988) 1634. R.P.F. Kanters, P.P.J. Schlebos, J.J. Bour, W.P. Bosman, J.M.M. Smits, P.T. Beurskens, J.J. Steggerda, Inorg. Chem. 29 (1990) 324.

[7] O.M. Abu-Salah, A.-R.A. Al-Ohaly, C.B. Knobler, J. Chem. Soc., Chem. Comm. (1985) 1502. O.M. Abu-Salah, A.R.A. Al-Ohaly, J. Chem. Soc., Dalton Trans. (1988) 2297.

[8] J.W.A. Velden, J.J. Bour, W.P. Bosman, J.H. Noordik, Inorg. Chem. 22 (1983) 1913.

[9] B.R. Sutherland, K. Folting, W.E. Streib, D.M. Ho, J.C. Huffman, K.G. Caulton, J. Am. Chem. Soc. 109 (1987) 3489.

[10] J.W. Lauher, K. Wald, J. Am. Chem. Soc. 103 (1981) 7648.

[11] J.G.M. Linden, A.M. Roelofsen, G.H.W. Ipskamp, Inorg. Chem. 28 (1989) 967.

[12] C.P. Blaxill, S.S.D. Brown, J.C. Frankland, I.D. Salter, V. Sik, J. Chem. Soc., Dalton Trans. (1989) 2039.

[13] B.K. Teo, X. Shi, H. Zhang, J. Am. Chem. Soc. 113 (1991) 4329.

[14] R. Reina, O. Rossell, M. Seco, J. Ros, R. Yáñez, A. Perales, Inorg. Chem. 30 (1991) 3973.

[15] B.F.G. Johnson, J. Lewis, W.J.H. Nelson, P.R. Traithby, M.D. Vargas, J. Chem. Soc., Chem. Comm. (1983) 608. Akhter, S.L. Ingham, J. Lewis, P.R. Raithby, Angew. Chem., Int. Ed. Engl. 35 (1996) 992.

[16] V.G. Albano, M.C. Iapalucci, G. Longoni, L. Manzi, M. Monari, Organometallics 16 (1997) 497.

[17] J. Ruiz, M.E.G. Mosquera, V. Riera, M. Vivanco, C. Bois, Organometallics 16 (1997) 3388.

[18] P.J. Fischer, V.G. Young, J.E. Ellis, J. Chem. Soc., Chem. Comm. (1997) 1249.

[19] P. Braunstein, J. Rose, Gold Bull. 18 (1985) 17 and references therein.

[20] J. Evans, G. Jingxing, J. Chem. Soc., Chem. Comm. (1985) 39.

[21] Y. Yuan, K. Asakura, H. Wan, K. Tsai, Y. Iwasawa, Chem. Lett. (1996) 129.

[22] A. Bauer, A. Schier, H. Schmidbaur, J. Chem. Soc., Dalton Trans. (1995) 2919.

[23] M. Linke, J.-C. Chambron, V. Heitz, J.-P. Sauvage, J. Am. Chem. Soc. 119 (1997) 11329.

[24] D. Li, X. Hong, C.-M. Che, W.-C. Lo, S.-M. Peng, J. Chem. Soc., Dalton Trans. (1993) 2929. S.-J. Shien, X. Hong, S.-M. Peng, C.-M. Che, J. Chem. Soc., Dalton Trans. (1994) 3067. B.-C. Tzeng, W.-C. Lo, C.-M. Che, S.-M. Peng, J. Chem. Soc., Chem. Comm. (1996) 181. B.-C. Tzeng, K.-K. Cheung, C.-M. Che, J. Chem. Soc., Chem. Comm. (1996) 1681.

[25] P. Pyykkö, W. Schneider, A. Bauer, A. Bayler, H. Schmidbaur, J. Chem. Soc., Chem. Comm. (1997) 1111. W. Schneider, A. Bauer, H. Schmidbaur, J. Chem. Soc., Dalton Trans. (1997) 415.

[26] M.J. Irwin, L.M. Rendina, J.J. Vittal, R.J. Puddephatt, J. Chem. Soc., Chem. Comm. (1996) 1281. M.J. Irwin, J.J. Vittal, G.P.A. Yap, R.J. Puddephatt, J. Am. Chem. Soc. 118 (1996) 13101.

[27] P.M.V. Calcar, M.M. Olmstead, A.L. Balch, J. Chem. Soc., Chem. Comm. (1995) 1773. D.V. Toronto, B. Weissbart, D.S. Tinti, A.L. Balch, Inorg. Chem. 35 (1996) 2484. P. Lange, A. Schier, H. Schmidbaur, Inorg. Chem. 35 (1996) 637. P.M.V. Calcar, M.M. Olmstead, A.L. Balch, Inorg. Chem. 36 (1997) 5231.

[28] D.M.P. Mingos, J. Yau, S. Menzer, D.J. Williams, Angew. Chem., Int. Ed. Engl. 34 (1995) 1894.

[29] A. Grohmann, Angew. Chem., Int. Ed. Engl. 34 (1995) 2107 and references therein.

[30] H. Schmidbaur, Chem. Soc. Rev. 24 (1995) 391 and references therein.

[31] (a) S. Onaka, M. Otsuka, A. Mizuno, S. Takagi, K. Sako, M. Otomo, Chem. Lett. (1994) 45. (b) S. Onaka, M. Otsuka, Chem. Lett. (1995) 2440. (c) S. Onaka, M. Otsuka, S. Takagi, K. Sako, J. Coord. Chem. 37 (1996) 151. (d) S. Onaka, Y. Katsukawa, S. Takagi, J. Organomet. Chem. 543 (1997) 241. (e) S. Onaka, Y. Katsukawa, M. Yamashita, J. Organomet. Chem. 564 (1998) 249. (f) S. Onaka, Y. Katuskawa, M. Shiotsuka, J. Organomet. Chem. 570 (1998) 113.

[32] S. Onaka, Y. Katsukawa, M. Yamashita, Chem. Lett. (1998) 525.

[33] D.T. Hill, G.R. Girard, F.L. McCabe, P.K. Johnson, P.D. Stupik, J.H. Zhang, W.M. Reiff, D.S. Eggleston, Inorg. Chem. 28 (1989) 3529.

[34] D.S. Eggleston, J.V. McArdle, G.E. Zuber, J. Chem. Soc., Dalton Trans. (1987) 677.

[35] C.A. McAuliffe, R.V. Parish, P.D. Randall, J. Chem. Soc., Dalton Trans. (1979) 1730.

[36] C.E. Coffey, J. Lewis, R.S. Nyholm, J. Chem. Soc. (1964) 1741. T.L. Blundell, H.M. Powell, J. Chem. Soc. (A) (1971) 1685.

[37] C. Katayama, Acta Crystallogr., Sect. A 42 (1986) 19.

[38] P.M.N. Low, Y.K. Yan, H.S.O. Chan, T.S.A. Hor, J. Organomet. Chem. 454 (1993) 205.

[39] S. Alvarez, O. Rossell, M. Seco, J. Valls, M.A. Pellinghelli, A. Tiripicchio, Organometallics 10 (1991) 2309.

[40] S.M. Draper, C.E. Housecroft, A.L. Rheingold, J. Organomet. Chem. 435 (1992) 9.

[41] J.R. Galsworthy, C.E. Housecroft, A.L. Rheingold, J. Chem. Soc., Dalton Trans. (1995) 2639.

[42] S. Onaka, T. Moriya, S. Takagi, A. Mizuno, H. Furuta, Bull. Chem. Soc. Jpn. 65 (1992) 1415. S. Onaka, A. Mizuno, S. Takagi, Chem. Lett. (1989) 2037.

[43] F.P. Gabbaï, A. Shier, J. Riede, H. Schmidbaur, Inorg. Chem. 34 (1995) 3855. F.P. Gabbaï, S.-C. Chung, A. Shier, S. Krüger, N. Rösch, H. Schmidbaur, Inorg. Chem. 36 (1997) 5699.

[44] P.G. Jones, Acta Crystallogr., Sect. B 36 (1980) 2775.

[45] J.B. Foley, A.E. Bruce, M.R.M. Bruce, J. Am. Chem. Soc. 117 (1995) 9596. P. Schwerdtfeger, A.E. Bruce, M.R.M. Bruce, J. Am. Chem. Soc. 120 (1998) 6587.

[46] H. Xiao, Y.-X. Weng, W.-T. Wong, T.C.W. Mak, C.-M. Che, J. Chem. Soc., Dalton Trans. (1997) 22.